PHYSICS OF PLASMAS VOLUME 9, NUMBER 9 SEPTEMBER 2002

Kinetic simulation of a quasisteady state in collisionless ion temperature gradient driven turbulence

Tomo-Hiko Watanabe and Hideo Sugama
National Institute for Fusion Science/The Graduate University for Advanced Studies, Toki, Gifu, 509-5292, Japan

(Received 21 May 2002; accepted 27 June 2002)

Existence of a quasisteady state with a mean transport flux in the collisionless ion temperature gradient driven turbulence has been confirmed by means of a direct numerical simulation of a basic kinetic equation for the perturbed ion velocity distribution function δf. The phase mixing generates fine-scale fluctuations of δf and leads to continuous growth of high-order moments which balances the transport flux. The phase relation between the temperature and the parallel heat flux is also examined and compared with a fluid closure model.
[DOI: 10.1063/1.1501823]

Turbulent transport in high-temperature plasmas has been a central subject in the fields of the magnetic fusion research.[1] Recent simulation studies based on the gyrokinetic and gyrofluid models[2] have revealed several important aspects of the ion/electron temperature gradient (ITG/ETG) driven turbulence,[3,4] where the main interest is taken in the nonlinear behaviors of low-order moments of the one-body velocity distribution function f (fluid variables such as density, fluid velocity, temperature and so on). This is related to the fact that the transport flux itself is described by correlations between these low-order moments and electromagnetic fields. It is, however, noteworthy that the fluid variables can not describe fine-scale fluctuations of f generated by the phase mixing, such as the ballistic mode.[5]

Details of the distribution function should be taken into account in the problems of steady transport caused by collisionless plasma turbulence. This is because, in order to observe an irreversible transport in a collisionless turbulence which is described by a basic kinetic equation with the time reversibility, one needs to extract a coarse-grained state from f with small-scale fluctuations. As pointed out by Krommes and Hu[6] and by Sugama *et al.*,[7,8] the entropy balance equation in slab ITG turbulence with periodic boundary condition is given by

$$\frac{d}{dt}(\delta S+W)=\eta_i Q_i\,, \tag{1}$$

where $\delta S\equiv\langle\int d^3v(\delta f)^2/2F_M\rangle$; $\langle\cdots\rangle$ and F_M, denote the spatial averaging and the Maxwellian distribution function, respectively; the potential energy W is defined in the wave number $\mathbf{k}$ space as $W=\Sigma_{\mathbf{k}}[1-\delta_{k_y,0}+(T_e/T_i)(1-\Gamma_0)]|\phi_{\mathbf{k}}|^2/2$ (see the next paragraph for definitions of Γ_0 and the perpendicular ion thermal flux Q_i). Here, the parallel nonlinear term is neglected by the gyrokinetic ordering and the adiabatic electron response is assumed. η_i is given by $\eta_i=L_n/L_T$, where L_n and L_T represent the density and temperature gradient scale lengths of the background ions with distribution F_M. δS is rewritten as $\delta S=S_M-S_m$ where $S_M=-\int d^3v\,F_M\ln F_M$ and $S_m=-\langle\int d^3v\,f\ln f\rangle$, with $f=F_M+\delta f$, represent macroscopic and microscopic entropy per unit volume, respectively. Regarding Eq. (1), one can consider two scenarios. One is a case with no mean transport $\overline{Q_i}=0$ in a *trivial* statistically steady state with $\overline{d(\delta S)/dt}=\overline{dW/dt}=0$, where $\overline{\cdots}$ means time averaging on a certain period, longer than characteristic times of the turbulence (scenario 1). Another one is a *quasisteady* state with a mean transport flux, $\overline{d(\delta S)/dt}=\eta_i\overline{Q_i}\neq 0$ with $\overline{dW/dt}=0$ (scenario 2). In the quasisteady state, continuous growth of fine-scale structures of δf in the velocity space (high-order moments of δf) contributes to monotonical increase of δS, while the low-order moments giving W and Q_i reach steady values. The latter case is more relevant to compare with the anomalous transport observed in experiments. The quasisteady state is regarded as an idealization of the real steady state where the high-order moments saturate as well due to collisional dissipation even if the collision frequency is much smaller than the characteristic ones of the turbulence.[8]

Our concern here is to confirm whether the quasisteady state could be realized in the collisionless slab ITG turbulence. For that purpose, we perform a direct numerical simulation for δf with the fine-scale fluctuations, where the basic kinetic equation is *directly* solved as a partial differential equation in the phase space (the so-called Vlasov simulation in literature) without use of an *ad hoc* model such as the finite-sized particle. In order to enable an accurate calculation of δf satisfying Eq. (1), the simulation code is implemented with high velocity space resolution and a nondissipative time integrator preserving the phase space integral of $(\delta f)^2$,[9] which had not been pursued in gyrokinetic[2,3] and conventional Vlasov[10] simulations. We employ a periodic two-dimensional slab configuration with translational symmetry in the z direction. The uniform magnetic field is written by $\mathbf{B}=B(\hat{z}+\theta\hat{y})$ where $\theta\ll 1$. The governing equations considered here are derived from the $v_\perp$ integral of gyrokinetic equations[11] by assuming $\delta f_{\mathbf{k}}(v_\parallel,v_\perp)=\tilde{f}_{\mathbf{k}}(v_\parallel)F_M(v_\perp)$. They are written in the wave number space $\mathbf{k}=(k_x,k_y)$ as

$$\partial_t \tilde{f}_{\mathbf{k}} + i\Theta v_\parallel k_y \tilde{f}_{\mathbf{k}} + \sum_{\mathbf{k}=\mathbf{k}'+\mathbf{k}''} (k_y' k_x'' - k_x' k_y'')\Psi_{\mathbf{k}'}\tilde{f}_{\mathbf{k}''}$$
$$= -ik_y \Psi_{\mathbf{k}}[1 + (v_\parallel^2 - 1 - k^2)\eta_i/2 + \Theta v_\parallel]F_M(v_\parallel) \tag{2}$$

and

$$[1 - \Gamma_0(k^2)]\phi_{\mathbf{k}} = e^{-k^2/2}\int \tilde{f}_{\mathbf{k}}(v_\parallel)dv_\parallel - \tilde{n}_{e,\mathbf{k}}, \tag{3}$$

where the electric potential $\phi_{\mathbf{k}}$ is related to $\Psi_{\mathbf{k}}$ by $\Psi_{\mathbf{k}} = e^{-k^2/2}\phi_{\mathbf{k}}$ with $k^2 = k_x^2 + k_y^2$. The above equations are normalized in the so-called gyrofluid units, such as $x = x'/\rho_i$, $y = y'/\rho_i$, $v = v'/v_{ti}$, $t = t' v_{ti}/L_n$, $\tilde{f} = \tilde{f}' L_n v_{ti}/\rho_i n_0$, and $\phi = e\phi' L_n/T_i\rho_i$, where v_{ti}, ρ_i, n_0, e, and T_i are the ion thermal velocity, the ion thermal gyroradius, the background plasma density, the elementary charge, and the background ion temperature ($T_i = m_i v_{ti}^2$; m_i means the ion mass), respectively. Prime means a dimensional quantity. Θ is defined as $\Theta = \theta L_n/\rho_i$. $\Gamma_0(k^2)$ is given by $\Gamma_0(k^2) = \exp(-k^2)I_0(k^2)$. $I_0(z)$ means the 0th modified Bessel function of z. Dorland and Hammett employed $\Gamma_0^{1/2}(k^2)$ for $\Psi_{\mathbf{k}}/\phi_{\mathbf{k}}$ instead of $e^{-k^2/2}$ in their finite-Larmor-radius closure model,[12] which gives the same linear dispersion relation as that in a full treatment of $\delta f_{\mathbf{k}}(v_\parallel, v_\perp)$. The difference between $e^{-k^2/2}$ and $\Gamma_0^{1/2}(k^2)$ is small for $k<1$. Furthermore, we drop $k_x = 0$ modes of $\tilde{f}_{\mathbf{k}}$ from computations, since they are included in the background part with constant density and temperature gradients in the x direction.[13] However, these conditions are not essential to the conclusion of the present study. We also assume the background electron temperature $T_e = T_i$ and the adiabatic electron response, such that $\tilde{n}_{e,\mathbf{k}} = \phi_{\mathbf{k}}$ for $k_y \neq 0$ and $\tilde{n}_{e,\mathbf{k}} = 0$ for $k_y = 0$. In this system, δS, W, and Q_i are, respectively, defined as $\delta S = \Sigma_{\mathbf{k}}\int dv_\parallel |\tilde{f}_{\mathbf{k}}|^2/2F_M(v_\parallel)$, $Q_i = \Sigma_{\mathbf{k}}\int dv_\parallel(-ik_y e^{-k^2/2}\phi_{\mathbf{k}})v_\parallel^2 \tilde{f}_{-\mathbf{k}}/2$, and $W = \Sigma_{\mathbf{k}}[1 - \delta_{k_y,0} + (T_e/T_i)(1-\Gamma_0)]|\phi_{\mathbf{k}}|^2/2$, which satisfy Eq. (1).

Employing the kinetic model described above, we have performed two types of simulations with and without the zonal flow components of $k_y = 0$. In the latter case, the $k_y = 0$ modes are artificially fixed to zero. In order to keep enough resolution for the phase mixing process, we have employed 8193 grid points for discretization of the velocity space, $-5 \leq v_\parallel \leq 5$. The minimum and maximum values of the wave number are set to be $k_{\min} = 0.1$ and $k_{\max} = 3.2$ for both of the k_x and k_y directions with the 3/2 rule for dealiasing in the spectral method. Exponential decay of $|\phi_{\mathbf{k}}|$ spectrum is observed for $k>1$, which ensures the convergence of the results.

The time evolutions of $d(\delta S)/dt$, dW/dt, and $-\eta_i Q_i$ for the case with the zonal flow are plotted in Fig. 1(a), where $\eta_i = 10$, $\Theta = 2.5$, and the time step $\Delta t = 0.0125$. For these parameters, the parallel phase velocity is -1.24 for the longest wavelength mode with $k_x = k_y = 0.1$ and -1.28 for the linearly most unstable mode with $k_x = 0.1$ and $k_y = 0.3$. In order to make the plot clear, fast time-scale fluctuations are eliminated in the figure by taking the running average of the results for a time period of $\tau = 5$. Since the zonal flow suppresses the turbulence after the peaking of the potential energy at $t \approx 160$, $d(\delta S)/dt$ and $\eta_i Q_i$ continue to decrease on

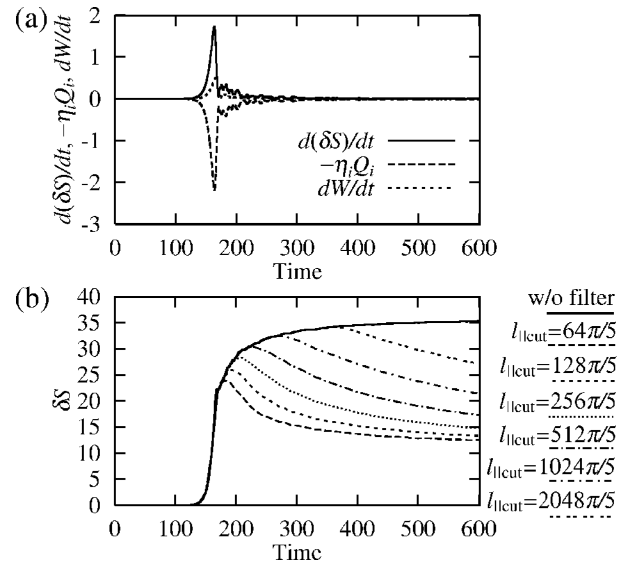

FIG. 1. Time histories of (a) $d(\delta S)/dt$, dW/dt, $-\eta_i Q_i$, (b) δS and its low-pass filtered values for $\eta_i = 10$ and $\Theta = 2.5$.

the average during the simulation run. In order to keep the velocity space resolution, the computation should be stopped when the velocity space scale of the ballistic mode reaches the grid size (at $t \approx 600$ for the present case and at $t \approx 800$ for the case without the zonal flow shown later). On the other hand, dW/dt fluctuates around zero, which shows that the potential fluctuations are statistically steady. The diffusion coefficient $\chi_i \equiv Q_i/\eta_i$ in the gyro-Bohm unit averaged around $t = 600$ is $\chi_i \approx 3 \times 10^{-5}\ \rho_i^2 v_{ti}/L_n$, and also continues to decrease in time. The final state in the case shown in Fig. 1(a) is, therefore, approximately regarded as the *trivial steady state* with no increase of δS and no thermal flux $[\overline{d(\delta S)/dt} = \eta_i \overline{Q_i} = 0]$, which corresponds to scenario 1. Even if the saturated flux is observed in a longer simulation run with a larger number of grids in the velocity space, the saturation level is expected to be negligibly small (at least $\chi_i < 3 \times 10^{-5}\ \rho_i^2 v_{ti}/L_n$). The time-history of δS is plotted by a solid line in Fig. 1(b), where dashed and dotted lines also indicate values of $\delta S_{\mathrm{cut}} = \Sigma_{\mathbf{k}}\int dv_\parallel |(\tilde{f}_{\mathbf{k}}/\sqrt{F_M})_{\mathrm{cut}}|^2/2$ that are calculated from the Fourier components of $\tilde{f}_{\mathbf{k}}(v_\parallel)/\sqrt{F_M(v_\parallel)}$ with the velocity-space wave numbers $l_\parallel$ of $|l_\parallel| \leq l_{\parallel\mathrm{cut}}$. δS_{cut} for lower $l_{\parallel\mathrm{cut}}$ peaks and starts to decay at earlier time, and then, stays at a smaller value. It means that the finer-scale fluctuations of $\tilde{f}_{\mathbf{k}}$ generated by the phase mixing have larger contributions to δS at later times of the simulation.

As shown in the above, the zonal flow excited by the turbulent stress suppresses the transport flux down to a quite small level, which is considered to be closely related to improved confinement such as the H-mode and the internal transport barrier.[14] Here, it should be recalled that, in a toroidal geometry, the zonal flow is severely damped by the collisionless transit time magnetic pumping effect.[15,16] Thus, χ_i observed in the L mode of a toroidal system is on a much higher level than that obtained in the above. Also, from the viewpoint of fluid modeling of kinetic effects on the turbulence saturation, it is valuable to examine how generation of

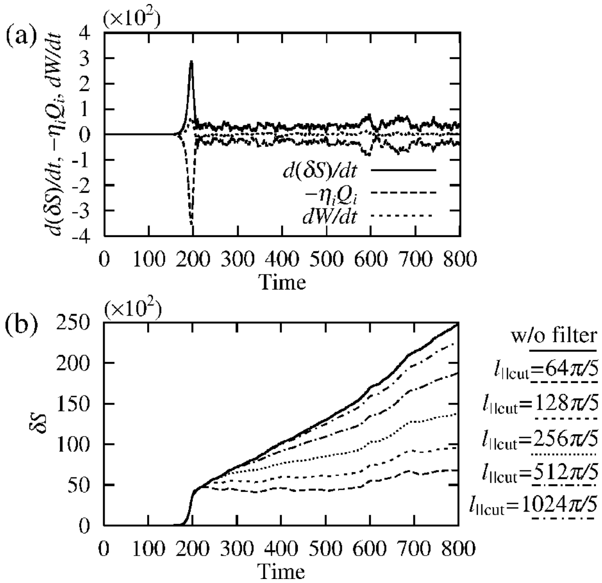

FIG. 2. Same as Fig. 1 but without the zonal flow.

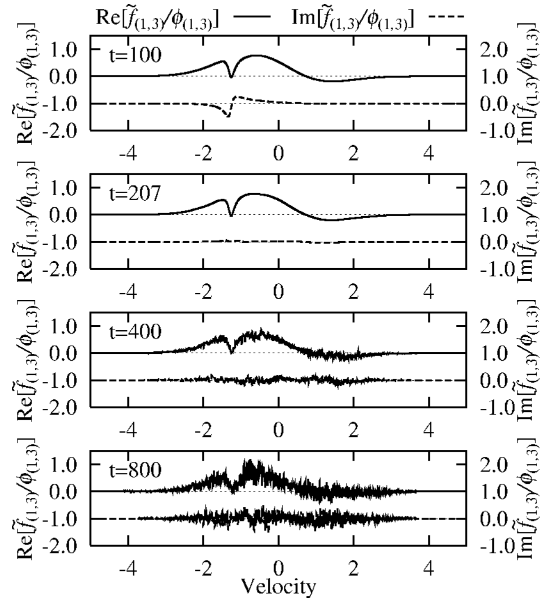

FIG. 3. Profiles of the perturbed distribution function of the linearly most unstable mode [$k_x=0.1$ and $k_y=0.3$; (1,3) mode] normalized by the potential at four different time steps for the case without the zonal flow.

fine-scale fluctuations of δf due to the phase mixing contributes to determination of a transport flux. In the following, therefore, in order to take account of the collisionless damping effect existing in toroidal systems, we consider the case without the zonal flow components.

In the absence of the zonal flow [see Fig. 2(a) where $\Delta t=6.25\times10^{-3}$; other parameters are the same as those in Fig. 1], the turbulence is enhanced by more than a hundred times of that shown in Fig. 1. $\overline{d(\delta S)/dt}$ and $\eta_i\overline{Q_i}$ apparently keep a constant level in the steady turbulence for low-order moments ($\overline{dW/dt}\approx0$), which corresponds to scenario 2. χ_i fluctuates around $\chi_i\approx0.36\,\rho_i^2 v_{ti}/L_n$. Since Eq. (1) is satisfied with the constant transport flux, δS linearly increases in time [see Fig. 2(b)]. More rapid growth of δS_{cut} is found for larger $l_{\parallel\mathrm{cut}}$, while δS_{cut} for smaller $l_{\parallel\mathrm{cut}}$ increases more slowly. In other words, the high-order moments of $\tilde{f}_{\mathbf{k}}$ continue to grow, while the low-order moments are steady on the average. It is, therefore, concluded that the *quasisteady* state is obtained in the simulation shown in Fig. 2.

Development of the fine-scale fluctuations is directly recognized in profiles of the distribution function in velocity space as shown in Fig. 3, where real and imaginary parts of $\tilde{f}_{\mathbf{k}}/\phi_{\mathbf{k}}$ of the linearly most unstable mode [$k_x=0.1$ and $k_y=0.3$ for the present parameters; this is called (1,3) mode, hereafter] are plotted at different time steps for the same case as in Fig. 2 without the zonal flow. During the linear growth, $\tilde{f}_{\mathbf{k}}/\phi_{\mathbf{k}}$ is represented by the linear eigenfunction $f_{L\mathbf{k}}$ for the normalized potential $\phi_{L\mathbf{k}}=1$ (see the plot at $t=100$ in Fig. 3). Even in the turbulent state, a coarse-grained form of $\mathrm{Re}(\tilde{f}_{\mathbf{k}}/\phi_{\mathbf{k}})$ is well approximated by $\mathrm{Re}(f_{L\mathbf{k}})$. On the other hand, after the peaking of the potential energy at $t\approx200$, the amplitude of the coarse-grained profile of $\mathrm{Im}(\tilde{f}_{\mathbf{k}}/\phi_{\mathbf{k}})$ is damped, and then, is governed by the fine-scale fluctuations. This means the correlations $\overline{\mathrm{Re}(ik_yT_{\mathbf{k}}\phi_{\mathbf{k}}^*)}$ and $\overline{\mathrm{Re}(ik_yT_{\mathbf{k}}q_{\mathbf{k}}^*)}$ almost vanish as discussed later, where $T_{\mathbf{k}}=\int dv_\parallel \tilde{f}_{\mathbf{k}}(v_\parallel^2-1)$ and $q_{\mathbf{k}}=\int dv_\parallel \tilde{f}_{\mathbf{k}}(v_\parallel^3-3v_\parallel)$. It is also suggested that the complex conjugate mode of the linear eigenfunction $f_{L\mathbf{k}}^*$ (Ref. 17) with a similar amplitude to that of $f_{L\mathbf{k}}$ is excited to cancel $\mathrm{Im}(\tilde{f}_{\mathbf{k}}/\phi_{\mathbf{k}})$. The result shown in Fig. 3 reminds us of the 3-mode ITG solution given by a linear combination of $f_{L\mathbf{k}}$ and $f_{L\mathbf{k}}^*$.[8,18]

Existence of the quasisteady state is a fundamental assumption in collisionless fluid closure models.[6,8] By comparing a balance equation similar to Eq. (1), which is obtained from equations of fluid moments, $n_{\mathbf{k}}=\int dv_\parallel \tilde{f}_{\mathbf{k}}$, $u_{\mathbf{k}}=\int dv_\parallel \tilde{f}_{\mathbf{k}} v_\parallel$, and $T_{\mathbf{k}}$, with that given by expanding Eq. (2) in the Hermite polynomials $H_n(v_\parallel)$ with the Maxwellian weight function, one finds[8]

$$\eta_i\overline{Q_i}=-\overline{\sum_{\mathbf{k}}\mathrm{Re}\left(\frac{ik_y\Theta}{2}T_{\mathbf{k}}q_{\mathbf{k}}^*\right)}=\overline{\frac{d}{dt}\sum_{\mathbf{k}}\sum_{n\geqslant4}\frac{n!}{2}|\varphi_{n\mathbf{k}}|^2}, \tag{4}$$

when the low-order ($n\leqslant3$) fluid moments are in the statistically steady state. Here, $\varphi_{n\mathbf{k}}$ denotes the nth coefficient of the Hermite polynomial expansion of $\tilde{f}_{\mathbf{k}}$. Equation (4) tells us that obtaining the steady transport in a collisionless system requires continuous growth of the higher-order moments (the quasisteady state). By taking the fluid moments of $\tilde{f}_{\mathbf{k}}$ shown in Fig. 3, we have found that Eq. (4) is approximately satisfied, that is, $-\overline{\sum_{\mathbf{k}}\mathrm{Re}(ik_y\Theta T_{\mathbf{k}}q_{\mathbf{k}}^*/2)}/\eta_i\overline{Q_i}\approx0.86$ where the time average is taken from $t=700$ to 800. The quasisteady state obtained by the present kinetic simulation provides the standard reference with which fluid simulations using the collisionless closure models should be compared.

As seen in Eq. (4), the phase relation between $T_{\mathbf{k}}$ and $q_{\mathbf{k}}$ is crucial in constructing a fluid closure model. In the Hammett–Perkins (HP) closure,[19] of which applicability is argued in comparison with other fluid models and kinetic approaches,[8,20] a constant phase angle is given by $\xi_{\mathbf{k}}\equiv\arg(q_{\mathbf{k}}/T_{\mathbf{k}})=-\pi/2$ for $k_y>0$ so that $-\mathrm{Re}(ik_yT_{\mathbf{k}}q_{\mathbf{k}}^*)$ is

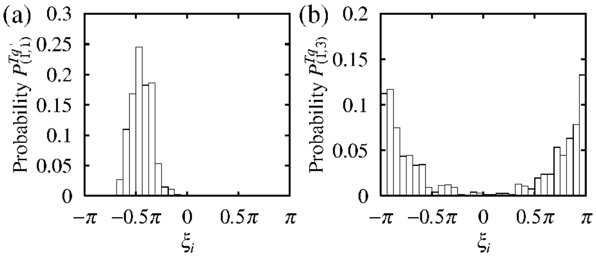

FIG. 4. Phase angle histograms of $T_{\mathbf{k}}$ and $q_{\mathbf{k}}$ for (a) the longest wavelength mode [$k_x=k_y=0.1$; (1,1) mode] and (b) the linearly most unstable mode [$k_x=0.1$ and $k_y=0.3$; (1,3) mode].

positive–definite. From the simulation results of $\tilde{f}_{\mathbf{k}}$ in the absence of the zonal flow, we have evaluated $\xi_{\mathbf{k}}$, of which histograms for the longest wavelength mode [$k_x=k_y=0.1$; this is called (1,1) mode] and the (1,3) mode are, respectively, shown in Figs. 4(a) and 4(b). The probability distribution $P^{Tq}_{\mathbf{k}}(\xi_i)$ in the histogram is defined as $P^{Tq}_{\mathbf{k}}(\xi_i)\equiv\int_{t_1}^{t_2}dt\int_{\xi_i-\Delta\xi/2}^{\xi_i+\Delta\xi/2}d\xi_{\mathbf{k}}A_{\mathbf{k}}(\xi_{\mathbf{k}})/\int_{t_1}^{t_2}dt\int_{-\pi}^{\pi}d\xi_{\mathbf{k}}A_{\mathbf{k}}(\xi_{\mathbf{k}})$, where $A_{\mathbf{k}}(\xi_{\mathbf{k}})=|T_{\mathbf{k}}||q_{\mathbf{k}}|$, $\Delta\xi=\pi/16$, and $\xi_i=-\pi+(i+\frac{1}{2})\Delta\xi$ with $i=0,1,\ldots,31$. The histogram of $\xi_{\mathbf{k}}$ taken from $t=t_1=700$ to $t=t_2=800$ for the (1,1) mode [Fig. 4(a)] peaks around $\xi_i=-\pi/2$ and is consistent with the HP closure model. On the other hand, an *oscillatory* phase relation is obtained for the (1,3) mode [Fig. 4(b)] where $\xi_{\mathbf{k}}$ peaks around $\pm\pi$ in contrast to the HP closure model. Thus, one observes the weak correlation of $-\overline{\mathrm{Re}(ik_yT_{\mathbf{k}}q^*_{\mathbf{k}})}/\overline{|k_yT_{\mathbf{k}}||q_{\mathbf{k}}|}\approx0.02$, while it is ≈0.94 for the (1,1) mode. The same tendency is found in the correlation for the transport flux, $\overline{\mathrm{Re}(ik_yT_{\mathbf{k}}\phi^*_{\mathbf{k}})}/\overline{|k_yT_{\mathbf{k}}||\phi_{\mathbf{k}}|}\approx-0.02$ for the (1,3) mode and ≈0.86 for the (1,1) mode. Thus, the linearly most unstable mode makes little contribution to the thermal transport, which is in contrast to conventional arguments based on the linear theory. These correspond to the result of the coarse-grained $\mathrm{Im}(\tilde{f}_{\mathbf{k}}/\phi_{\mathbf{k}})\sim0$ shown in Fig. 3.

Concerning the closure relation, it is also noteworthy that the linearly stable modes with $|\mathbf{k}|\geqslant0.7$ have a major contribution to the sum of products of $k_yT_{\mathbf{k}}$ and $q^*_{\mathbf{k}}$ such as $\overline{\Sigma_{|\mathbf{k}|\geqslant0.7}\mathrm{Re}(ik_yT_{\mathbf{k}}q^*_{\mathbf{k}})}/\overline{\Sigma_{\mathbf{k}}\mathrm{Re}(ik_yT_{\mathbf{k}}q^*_{\mathbf{k}})}\approx0.7$ where the time average is taken from $t=700$ to 800. The (1,1) mode, however, dominates in producing the transport flux, $\overline{\mathrm{Re}(ik_yT_{\mathbf{k}}e^{-k^2/2}\phi^*_{\mathbf{k}}/2)}/\overline{Q_i}\approx0.85$. It implies that $|f_{\mathbf{k}}|^2$ is nonlinearly transferred from the long to the short wavelength modes.

In summary, by means of direct numerical simulations of δf, we have confirmed existence of the quasisteady state with a mean transport flux in the strongly driven collisionless ITG turbulence. The phase mixing plays a key role in generating the fine-scale fluctuations in the velocity space and in increasing the functional δS. It is currently examined how the observed properties of the coarse-grained distribution function depend on the parameters η_i and Θ. The obtained phase relations between the fluid variables show disagreement with those of the HP model for the linearly most unstable mode, and motivate other closure methods such as the nondissipative closure model (NCM)[8] which includes the case of $\mathrm{Im}(\tilde{f}_{\mathbf{k}}/\phi_{\mathbf{k}})\sim0$. Comparison between the kinetic simulation and the NCM fluid simulation results is in progress and will be reported elsewhere.

ACKNOWLEDGMENTS

The authors would like to thank Y. Todo, T. Sato, and W. Horton for their fruitful comments and discussions. Numerical computations are performed on the NIFS MISSION System.

This work is partially supported by grants-in-aid of the Ministry of Education, Culture, Sports, Science and Technology (No. 12680497 and 14780387).

[1] W. Horton, Rev. Mod. Phys. **71**, 735 (1999).
[2] A. M. Dimits, G. Bateman, M. A. Beer *et al.*, Phys. Plasmas **7**, 969 (2000).
[3] Z. Lin, T. S. Hahm, W. W. Lee, W. M. Tang, and R. B. White, Science **281**, 1835 (1998).
[4] W. Dorland, F. Jenko, M. Kotschenreuther, and B. N. Rogers, Phys. Rev. Lett. **85**, 5579 (2000).
[5] N. A. Krall and A. W. Trivelpiece, *Principles of Plasma Physics* (McGraw-Hill, New York, 1973), p. 393.
[6] J. A. Krommes and G. Hu, Phys. Plasmas **1**, 3211 (1994).
[7] H. Sugama, M. Okamoto, W. Horton, and M. Wakatani, Phys. Plasmas **3**, 2379 (1996).
[8] H. Sugama, T.-H. Watanabe, and W. Horton, Phys. Plasmas **8**, 2617 (2001).
[9] T.-H. Watanabe, H. Sugama, and T. Sato, J. Phys. Soc. Jpn. **70**, 3565 (2001).
[10] G. Manfredi, M. Shoucri, R. O. Dendy, A. Ghizzo, and P. Bertrand, Phys. Plasmas **3**, 202 (1996).
[11] D. H. E. Dubin, J. A. Krommes, C. Oberman, and W. W. Lee, Phys. Fluids **26**, 3524 (1983).
[12] W. Dorland and G. W. Hammett, Phys. Fluids B **5**, 812 (1993).
[13] W. W. Lee, J. Comput. Phys. **72**, 243 (1987).
[14] P. W. Terry, Rev. Mod. Phys. **72**, 109 (2000).
[15] T. H. Stix, Phys. Fluids **16**, 1260 (1973).
[16] Z. Lin, T. S. Hahm, W. W. Lee, W. M. Tang, and R. B. White, Phys. Plasmas **7**, 1857 (2000).
[17] It is known that $f^*_{L\mathbf{k}}\exp(-i\omega^*_{L\mathbf{k}}t)$, where $\omega_{L\mathbf{k}}$ is the complex eigenfrequency, is a solution of an initial value problem for a linearized version of Eq. (2), if the normal mode solution is unstable (Ref. 8).
[18] T.-H. Watanabe, H. Sugama, and T. Sato, Phys. Plasmas **7**, 984 (2000).
[19] G. W. Hammett and F. W. Perkins, Phys. Rev. Lett. **64**, 3019 (1990).
[20] N. Mattor, Phys. Fluids B **4**, 3952 (1992).